The Journal of Infectious Diseases

MAJOR ARTICLE

An RSV Live-Attenuated Vaccine Candidate Lacking G Protein Mucin Domains Is Attenuated, Immunogenic, and Effective in Preventing RSV in BALB/c Mice

Molly K. Roe,[1] Maria A. Perez,[2,3] Hui-Mien Hsiao,[2,3] Stacey A. Lapp,[2,3] He-Ying Sun,[2,3] Samadhan Jadhao,[2,3] Audrey R. Young,[1] Yara S. Batista,[1] Ryan C. Reed,[4] Azmain Taz,[4] Anne Piantadosi,[4] Xuemin Chen,[2,3] Bo Liang,[5] Michael Koval,[4] Timothy A. Snider,[6] Martin L. Moore,[7] Evan J. Anderson,[2,3,4] Larry J. Anderson,[2,3] Christopher C. Stobart,[1] and Christina A. Rostad[2,3]

[1]Department of Biological Sciences, Butler University, Indianapolis, Indiana, USA; [2]Department of Pediatrics, Emory University School of Medicine, Atlanta, Georgia, USA; [3]Center for Childhood Infections and Vaccines, Children's Healthcare of Atlanta and Emory University School of Medicine, Atlanta, Georgia, USA; [4]Department of Medicine, Emory University School of Medicine, Atlanta, Georgia, USA; [5]Department of Biochemistry, Emory University School of Medicine, Atlanta, Georgia, USA; [6]Department of Veterinary Pathobiology, Oklahoma State University, Stillwater, Oklahoma, USA; and [7]Meissa Vaccines, Inc, Redwood City, California, USA

Background. Respiratory syncytial virus (RSV) is a leading viral respiratory pathogen in infants. The objective of this study was to generate RSV live-attenuated vaccine (LAV) candidates by removing the G-protein mucin domains to attenuate viral replication while retaining immunogenicity through deshielding of surface epitopes.

Methods. Two LAV candidates were generated from recombinant RSV A2-line19F by deletion of the G-protein mucin domains (A2-line19F-G155) or deletion of the G-protein mucin and transmembrane domains (A2-line19F-G155S). Vaccine attenuation was measured in BALB/c mouse lungs by fluorescent focus unit (FFU) assays and real-time polymerase chain reaction (RT-PCR). Immunogenicity was determined by measuring serum binding and neutralizing antibodies in mice following prime/boost on days 28 and 59. Efficacy was determined by measuring RSV lung viral loads on day 4 postchallenge.

Results. Both LAVs were undetectable in mouse lungs by FFU assay and elicited similar neutralizing antibody titers compared to A2-line19F on days 28 and 59. Following RSV challenge, vaccinated mice showed no detectable RSV in the lungs by FFU assay and a significant reduction in RSV RNA in the lungs by RT-PCR of 560-fold for A2-line19F-G155 and 604-fold for A2-line19F-G155S compared to RSV-challenged, unvaccinated mice.

Conclusions. Removal of the G-protein mucin domains produced RSV LAV candidates that were highly attenuated with retained immunogenicity.

Keywords. RSV; glycoprotein; glycosylation; live-attenuated vaccine; mucin domains; pediatric.

Respiratory syncytial virus (RSV) is a major human respiratory pathogen and a leading cause of infant morbidity worldwide, infecting most children by the age of 2 years [1]. In 2019, 3.6 million hospital admissions were associated with acute lower respiratory infections due to RSV worldwide, and 39% of these occurred in infants ≤6 months of age with 101 400 RSV-attributable deaths [2]. During the coronavirus disease 2019 (COVID-19) pandemic, a quiescent respiratory viral season in 2020 was followed by a delayed seasonal surge of RSV in the summer of 2021 [3], underscoring the ongoing need for an effective RSV vaccine. Early attempts to pioneer an RSV vaccine by formalin inactivation in the 1960s not only failed to reduce infection, but instead primed for enhanced disease in RSV-naive recipients upon natural infection [4]. Enhanced disease has not been observed following live-attenuated vaccines (LAVs) [5], and LAVs have therefore been regarded as a preferred method to safely vaccinate the target population of RSV-naive infants. Unfortunately, balancing attenuation with immunogenicity in LAVs remains challenging, and no RSV vaccine has been licensed to date [6, 7].

RSV is an enveloped, negative-sense, single-stranded RNA virus, belonging to the Pneumoviridae family, and the *Orthopneumovirus* genus. Its genome contains 10 genes encoding 11 known proteins. Among these, the surface glycoproteins F (which mediates viral fusion) and G (which facilitates attachment) are the predominant immunogens, capable of eliciting neutralizing antibodies in vivo [8–10]. G is a heavily glycosylated 298-amino acid protein, which consists of 2 large, variable, mucin-like domains that flank a highly conserved CX3C motif within the central conserved domain (CCD). G is the most

Received 09 May 2022; editorial decision 14 September 2022; accepted 31 October 2022; published online 25 October 2022

Presented in part: St Jude Pediatric Infectious Diseases Society Conference, March 3–5, 2022 in Memphis, TN, USA.

Correspondence: Christina A. Rostad, MD, Emory Children's Center, 2015 Uppergate Drive NE, Atlanta, GA 30322 (christina.rostad@emory.edu).

The Journal of Infectious Diseases® 2023;227:50–60

https://doi.org/10.1093/infdis/jiac382

variable protein of RSV, and the majority of diversity between RSV strains lies within the G-mucin domains. G exists in transmembrane bound and secreted forms, and the secreted form may function as an antigen decoy, interfering with antibody-mediated immune responses [11]. While deletion of the entire G protein attenuates viral replication, the role of the G-mucin domains has not been fully characterized [12].

The glycosylated regions of some viral glycoproteins can function as steric shields, masking surface epitopes from recognition by the host immune system and facilitating immune evasion [13, 14]. We therefore hypothesized that removal of the heavily glycosylated mucin domains from RSV G would generate a highly attenuated vaccine candidate with impaired viral attachment but preserved immunogenicity due to deshielding of immunodominant epitopes.

METHODS

Cell Culture

HEp-2, Vero, and BSR-T7/5 cells were cultured as previously described [15]. The recombinant viruses analyzed in this study express monomeric Katushka 2 (mKate2), a far-red fluorescent reporter protein located in the first gene position. Previous studies indicated recombinant expression of mKate2 did not cause viral attenuation [6, 16].

Primary normal human bronchial epithelial (NHBE) cells were isolated from human donor lung explants under an institutional review board-approved protocol and cultured at an air-liquid interface (ALI) as previously described [17]. In brief, cells were expanded in coculture with irradiated 3T3 cells in F + Y Reprogramming Medium and then plated on Costar 3470 plates (0.4 μM pore size, polyester; Corning). After 2 days the cells were transitioned to ALI and differentiated in E-ALI medium [17]. Once cultures were at ALI, the medium was changed every 48–72 hours and cultures were allowed to differentiate for at least 3 weeks before experimentation.

Assembly and Rescue of Recombinant RSV Viruses

The rescue of recombinant A2-line19F, which expresses mKate2 and the RSV strain line19 fusion protein in an A2 backbone, was previously described [16]. To generate recombinant viruses expressing modified G proteins within the A2-line19F backbone, synthetic G nucleotide sequences were obtained from GenScript, flanked by SacI-SacII restriction sites that were used to clone the corresponding G genes into the pSynkRSV-A2-line19F bacterial artificial chromosome. The resultant strain A2-line19F-G155 had deletion of the G-protein mucin domains, whereas strain A2-line19F-G155S had deletion of both the G protein mucin domains and the transmembrane domain such that it only expressed a secreted G protein lacking mucin (Figure 1 and Figure 2). To recover the recombinant viruses, BSR-T7/5 cells were cotransfected with RSV antigenomic bacterial artificial chromosomes and 4 human codon-optimized helper plasmids expressing either RSV N, P, M2-1, and L, as previously described [16, 18]. Master and working virus stocks were generated and harvested from Vero cells, flash-frozen in liquid nitrogen, and stored at −80°C until use. RNA from viral stocks was extracted (RNeasy; QIAGEN) and the F and G genes were sequence confirmed by Sanger sequencing. Whole viral genome sequencing (Supplementary Methods and Supplementary Table 1) confirmed the entire sequence identify of A2-line19F-G155 and identified a single mutation in A2-line19F-G155S large polymerase protein gene that resulted in a K1766E amino acid change that did not lie within a functionally active or conserved domain [19].

Characterization of Protein Expression

The protein structures of the G mutants compared to wild-type A2G were modeled using Phyre2 and AlphaFold version 2.1.0, and graphics were generated by PyMOL Molecular Graphics System version 1.7.6.3 (Schrödinger, LLC) (Figure 2) [20, 21]. To measure protein expression, western blots were performed on infected HEp-2 lysates and supernatants (Supplementary Methods). Monoclonal antibody binding of motavizumab (anti-F) and 3D3 (anti-G) to whole virus was also measured using an enzyme-linked immunosorbent assay (ELISA) (Supplementary Methods).

Surface expression of F and G on infected cells was measured by immunofluorescence using flow cytometry. HEp-2 cells were infected with A2-line19F or the vaccine strains and incubated at 37°C overnight. The following day, cells were incubated with motavizumab and 3D3 monoclonal antibodies and subsequently stained with allophycocyanin-conjugated goat anti-human IgG (H + L) antibody (No. 109-136-098; Jackson ImmunoResearch Laboratory) and Brilliant Violet 421 goat anti-mouse IgG (No. 405317; BioLegend) for 30 minutes. Images were acquired on an LSR II flow cytometer (BD Biosciences) and analyzed with FlowJo software (Tree Star). Gating was performed on live cells and singlets, and infected cells were gated based on mKate2 expression (Figure 3).

Viral Replication In Vitro

To measure viral growth kinetics in vitro, 6-well plates containing Vero cells at 70%–90% confluency were infected in duplicate at a multiplicity of infection (MOI) of 0.01 in 500 μL/well as previously described [15]. At hours 6, 24, 48, 72, 96, and 120 postinfection, cell monolayers were scraped into supernatant, vortexed, flash-frozen in liquid nitrogen, and stored at −80°C until titrating.

NHBE cells differentiated at ALI were infected in triplicate at MOI of 8.0 based on a seeded cell density of 150 000 at 100 μL/insert. Cells were washed with Emory-ALI medium, and virus inoculum was applied apically for 2 hours at 37°C. At hours 0 and 24, 48, 72, 96, and 120 postinfection, 150 μL full medium

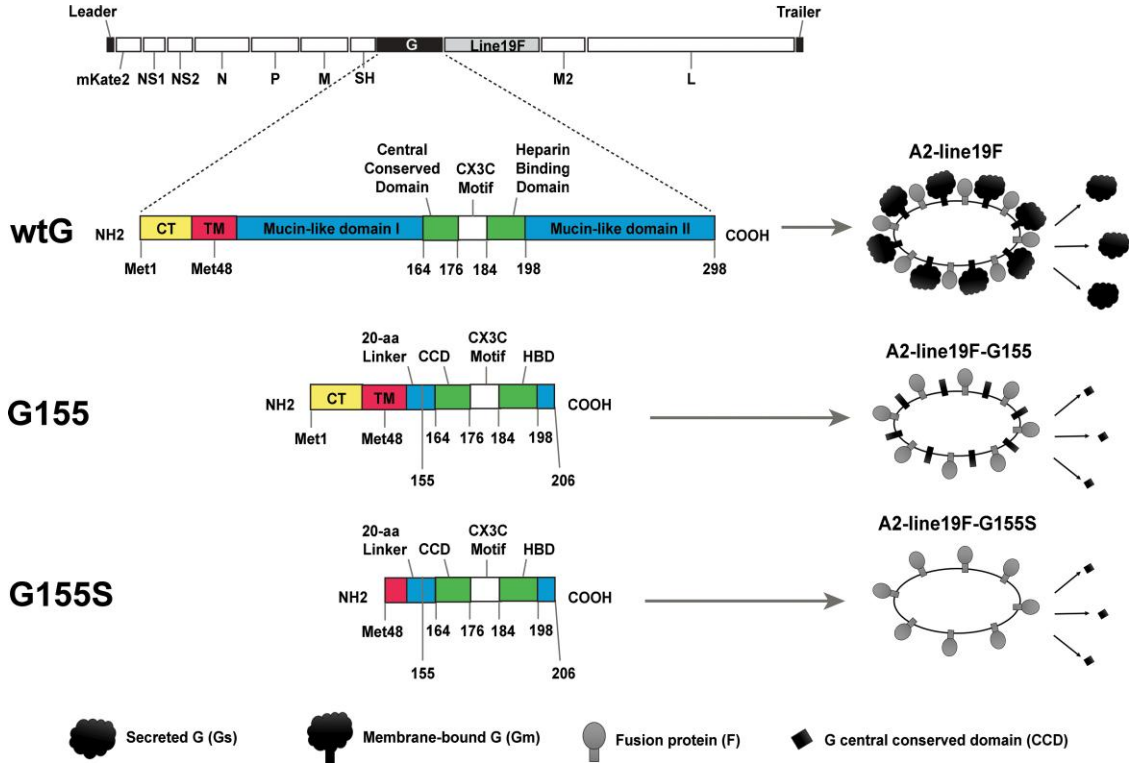

Figure 1. Schematic of RSV wild-type A2-line19 and G-mutant vaccines. A2-line19F is wild-type A2 virus with a substituted thermostable fusion protein gene from the line19 strain. A2-line19F-G155 has a deletion that removes the mucin domains from G protein. A2-line19F-G155S additionally has removal of the G protein transmembrane domain sequence. Thus, this strain expresses a G protein limited to the CCD, which is exclusively secreted (no membrane-bound G). Numbers represent amino acid residues in wild-type A2 G protein. Abbreviations: aa, amino acid; CCD, central conserved domain; COOH, C-terminal domain; CT, cytoplasmic tail; HBD, heparin binding domain; Met, methionine; NH2, N-terminal domain; RSV, respiratory syncytial virus; TM, transmembrane domain; wtG, wild-type G.

was applied apically twice for 10 minutes at 37°C. The 300 µL/insert was flash-frozen in liquid nitrogen and stored at −80°C until titrating. Virus titers were determined using a fluorescent focus unit (FFU) quantification assay 48 hours postinfection on HEp-2 cells as previously described [7].

Animal Studies

Six- to 8-week-old female BALB/c mice obtained from the Jackson Laboratory (Bar Harbor, ME) were housed under pathogen-free conditions until the time of use. All animal experiments were performed with approval of the Emory University Institutional Animal Care and Use Committee.

Viral Replication of G-Mutant Vaccines in BALB/c Mice

To ascertain the level of viral attenuation in vivo, we infected groups of 5 BALB/c mice intranasally (IN) with 10^6 FFU of A2-line19F, A2-line19F-G155, or A2-line19F-G155S under ketamine/xylazine anesthesia. On day 4 postinfection, we euthanized the mice using pentobarbital, harvested the left lung, homogenized, and measured lung viral load using the FFU assay and real-time polymerase chain reaction (RT-PCR) (Supplementary Methods). The ΔCt (difference in cycle threshold) between the RSV matrix M (gene of interest) and glyceraldehyde-3-phosphate dehydrogenase (*GAPDH*; endogenous control) genes were calculated for each sample and averaged for 2 replicates. The ΔΔCt (difference between each sample's ΔCt and the mean positive control [A2-line19F] ΔCt) was calculated to determine viral replication relative to A2-line19F. The linear fold-change in RSV M gene expression levels for a given sample relative to A2-line19F was calculated using the formula $2^{(-\Delta\Delta Ct)}$.

Immunogenicity of G Mutants in BALB/c Mice

To ascertain immunogenicity of the G-mutant vaccines in BALB/c mice, we infected groups of 5 BALB/c mice IN with 10^6 FFU of A2-line19F, A2-line19F-G155, A2-line19F-G155S, or mock (plain minimum essentials medium [MEM]) with a prime/boost regimen on days 1 and 29 (Supplementary Figure 2). Another group of mice had intramuscular administration of 50 µL of formalin-inactivated A2-line19F (FI-RSV) (Supplementary Methods) at the same time points. Serum was collected by submandibular bleeding on days 0, 28, and 59. For the wellbeing of the animals, the blood collection was performed on the day preceding vaccination or challenge rather than the same day. Samples were centrifuged at 8000*g* for 10 minutes, the supernatant removed, pooled for each group, heat-inactivated at 56°C for 30 minutes, and stored at −80°C until testing.

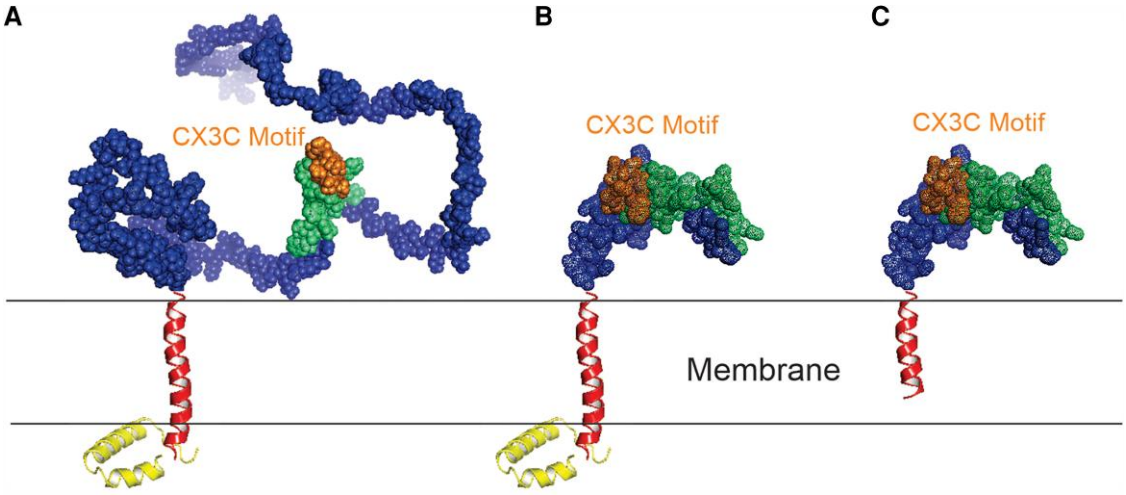

Figure 2. The structural comparisons of wild-type A2 G protein and G mutants with deleted mucin domains. The modeled protein structures of (*A*) A2 G; (*B*) G155 (with deleted mucin domains); and (*C*) G155S (with deleted mucin domains and transmembrane domain). The color scheme is the same as Figure 1, except that the CX3C motif is highlighted in gold. The structures were modeled with Phyre2 and AlphaFold 2.1.0, and the graphics were generated by PyMOL Molecular Graphics System, version 1.7.6.3 (Schrödinger, LLC).

To measure immunogenicity, mouse sera were analyzed by ELISA for binding antibodies to RSV full-length A2-F, prefusion stabilized A2-F, and G CCD peptide (Supplementary Methods); and by neutralization assays to A2-line19F. RSV F and G CCD were analyzed as single replicates due to limitations in sample volume, whereas RSV prefusion F was analyzed in 2 replicates and the GMT end-point titer determined. Neutralization assays were performed as previously described [15]. Fifty percent maximum effective concentration (EC_{50}) values were generated, and the GMT of 2 replicates of each pooled specimen was determined.

Vaccine Efficacy of G Mutants in BALB-c Mice

To determine vaccine efficacy against RSV challenge, the same mice described above were then challenged with 10^6 FFU IN of A2-line19F on day 60. Four days after challenge, the mice were euthanized and the left lungs were harvested and homogenized for viral titration by FFU assay and RT-PCR. RT-PCR was performed analogously to the mouse lung attenuation experiment detailed above, with exception that the ΔΔCt between each sample's ΔCt and the mean mock ΔCt was calculated to determine viral replication relative to mock.

To determine the potential for the vaccines to elicit enhanced histopathology after RSV challenge, the right lungs were also excised at the time of euthanasia and placed in 10% neutral buffered formalin. Samples were embedded in paraffin, 4-μm sections were cut, and stained with hematoxylin and eosin. Histopathologic scores were performed by a blinded veterinary pathologist (T. A. S.) for 3 parameters as previously described: eosinophil recruitment, perivascular cuffing, and interstitial pneumonia [22]. A fourth parameter of pulmonary edema was added. Each parameter was scored separately for each histopathologic section, with a maximum value of 4 and a minimum of 0. Immunohistochemistry staining was also performed to ascertain the presence of RSV antigen in the lungs using goat polyclonal anti-RSV antibody (No. AB1128, Sigma-Aldrich).

Statistical Analyses

Statistical comparisons were made using 1- or 2-way analysis of variance (ANOVA) with Tukey post hoc comparison test using GraphPad Prism version 8.0. For viral titers and antibody titers, the $\log_{10}$-transformation of the titers were statistically compared. P values $\leq .05$ were considered statistically significant.

RESULTS

Confirmation of RSV F and G Expression in G-Mutant Viruses by Western Blotting

The presence of the F and G proteins was measured by western blotting in both cellular lysate and supernatant for each viral strain, utilizing RSV nucleoprotein (N) protein as a loading control (Supplementary Figure 1*A* and 1*B*). Results for A2-line19F and A2-line19F-G155 indicated the G protein's presence primarily in the lysate. In contrast, A2-line19F-G155S had minimal G protein expression in the lysate, but was detectable in higher quantities in the supernatant, consistent with the deletion of the G protein transmembrane domain. F was present only in the lysate, with comparable expression levels by each strain when normalized to N protein expression.

RSV F and G Protein Binding of G-Mutant Viruses

To determine if the removal of G-mucin domains resulted in increased accessibility to antibody binding of RSV surface

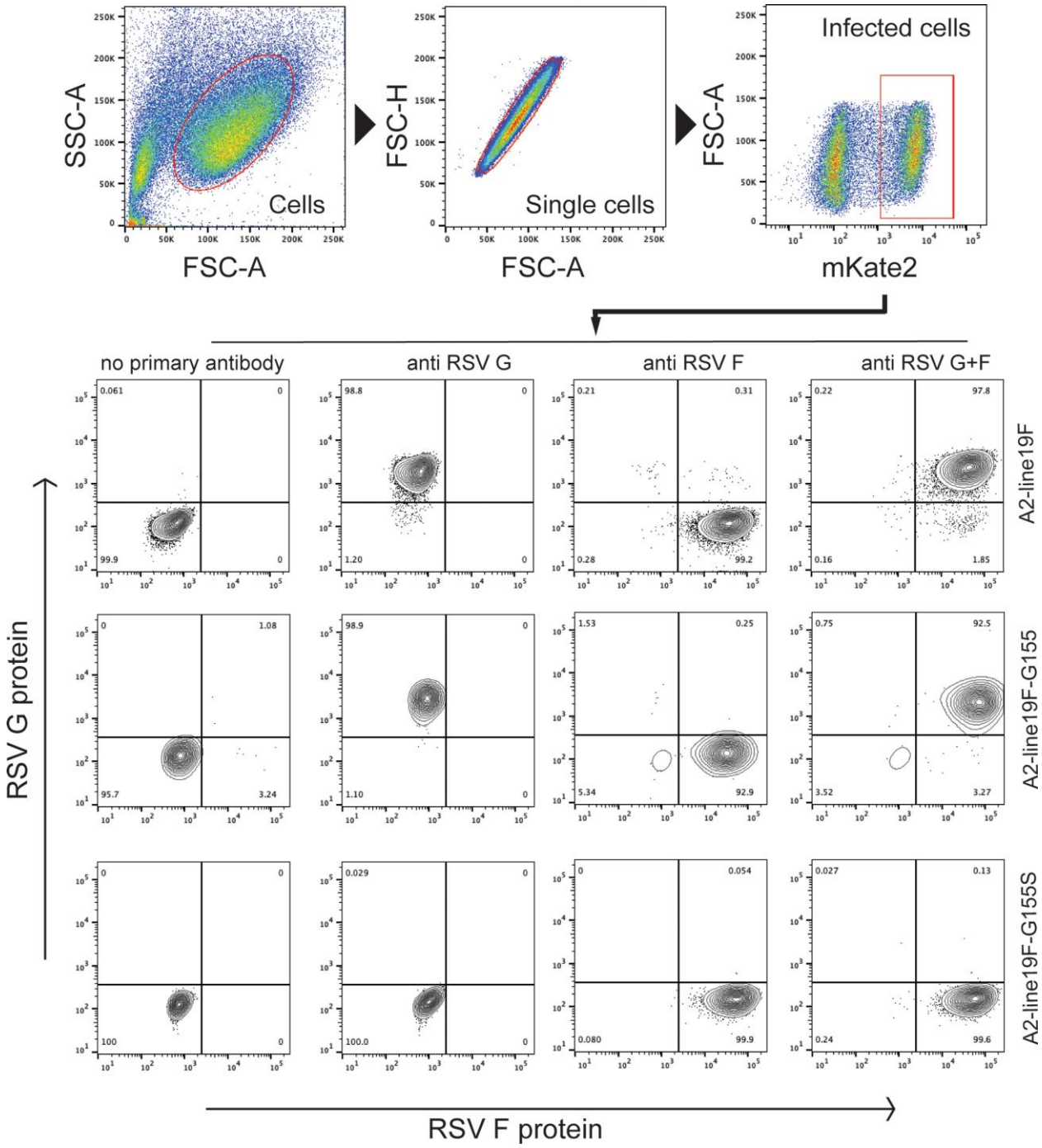

Figure 3. Surface F and G expression on HEp-2 cells infected with RSV G-mutant vaccines by flow cytometry. Gating was performed on live cells and singlets, and infected cells were gated based on mKate2 expression. Reactivity of RSV F (motavizumab) and G (3D3) monoclonal antibodies was measured using immunofluorescence. Abbreviations: FSC, forward scatter; RSV, respiratory syncytial virus; SSC, side scatter.

proteins, we performed ELISA analyses using motavizumab and 3D3 binding to F and G, respectively, to whole virus stock (Supplementary Figure 1C). Despite relatively similar F protein expression levels by each strain (demonstrated by western blot), A2-line19F-G155 and A2-line19F-G155S both demonstrated a higher level of monoclonal antibody binding to F protein than A2-line19F. In contrast, G monoclonal antibody binding (3D3) was similar for A2-line19F and A2-line19F-G155, but significantly lower for A2-line19F-G155S, consistent with the lack of membrane-bound G expression on its surface.

Flow Cytometry of Surface Glycoproteins

Surface F and G expression were measured by immunofluorescence using flow cytometry of infected HEp-2 cells (Figure 3). As expected, cells infected with A2-line19F-G155S lacked surface G expression, attributable to deletion of the G transmembrane domain. Cells infected with either vaccine candidate or wild-type demonstrated surface expression of F with similar median fluorescent intensity (37 258 for A2-line19F, 42 239 for A2-line19F-G155, and 41 132 for A2-line19F-G155S).

Growth Kinetics of G-Mutant Viruses

To assess the impact of the removal of mucin domains on viral growth kinetics in vitro, we then infected Vero cells (Figure 4*A*) and NHBE cells differentiated at ALI (Figure 4*B*). Both A2-line19F-G155 and A2-line19F-G155S grew to similar titers as A2-line19F in Vero cells. However, in NHBE cells at ALI, which best approximate viral growth kinetics in seronegative infants [23], the vaccine candidates were significantly attenuated compared to both A2 and A2-line19F.

Viral Growth Kinetics in BALB/c Mice

To measure the level of vaccine attenuation in vivo, we then infected groups of 5 BALB/c mice IN with 10^6 FFU of either A2-line19F, A2-line19F-G155, or A2-line19F-G155S. On day 4 postinfection, mice were euthanized, lungs were harvested and homogenized, and viral lung titer was measured by FFU assay (Figure 4*C*) and RT-PCR (Figure 4*D*). By the live-virus FFU assay, A2-line19F-G155 and A2-line19F-G155S were undetectable in the mouse lungs, as compared to A2-line19F, which had a geometric mean titer (GMT) of 4.62 $\log_{10}$ FFU/g lung (fold-reduction >124-fold). By RT-PCR, which also has the potential to detect nonreplicating viral RNA, detection as measured by Ct fold-change was reduced 3-fold for A2-line19F-G155S and 22-fold for A2-line19F-G155 compared to A2-line19F.

Immunogenicity of G Mutants in BALB/c Mice

We then measured the immunogenicity of the vaccine candidates in BALB/c mice using a prime/boost regimen on days 1 and 29, vaccinating mice with A2-line19F-G155, A2-line19F-G155S, A2-line19F, mock, or FI-RSV (intramuscular) and challenging with RSV A2-line19F on day 60 (Supplementary Figure 2). Binding and neutralizing antibody responses were measured by RSV F ELISA (Supplementary Figure 3*A*), RSV G-CCD ELISA (Supplementary Figure 3*B*), RSV prefusion F ELISA (Figure 5*A*), and neutralizing antibodies to A2-line19F in HEp-2 cells (Figure 5*B*). We found that A2-line19F-G155 and A2-line19F-G155S vaccines elicited similar levels of RSV F and prefusion F binding antibodies compared to A2-line19F on days 28 and 59. In contrast, binding antibodies to the G-CCD elicited by the vaccine candidates were numerically lower than those elicited by A2-line19F or FI-RSV. Both vaccine candidates elicited similar titers of neutralizing antibodies compared to A2-line19F on day 28. Neutralizing antibody titers significantly increased with the boost dose of vaccination, regardless of the priming vaccine.

Vaccine Efficacy of G Mutants in BALB/c Mice

To assess for vaccine efficacy, these same mice were then challenged IN with 10^6 FFU of A2-line19F on day 60 and the left lungs were harvested 4 days postchallenge. Both G-mutant vaccines reduced lung viral titers to undetectable levels by FFU assay after RSV challenge, comparable to wild-type A2-line19F and FI-RSV (Figure 5*C*). By RT-PCR, vaccination reduced lung viral RNA detection 560-fold for A2-line19F-G155, 604-fold for A2-line19F-G155S, and 1812-fold for A2-line19F when compared to mock-challenged mice (Figure 5*D*).

Lung Histopathology Postchallenge

To assess for lung histopathology after challenge, the same mice who were challenged with 10^6 FFU IN of A2-line19F on day 60 had the right lungs harvested for histopathological analysis and stained with hematoxylin and eosin. Immunohistochemistry demonstrated the presence of RSV antigen in all lung samples of mice challenged with A2-line19F (data not shown). Blinded histopathologic analysis demonstrated that mice primed/boosted with FI-RSV IM had significantly worse combined histopathological scores on day 4 postchallenge (mean score 9.2, SD 1.3) than all other groups (Figure 6; $P < .005$ for all comparisons). The mean histopathologic scores of mice vaccinated with A2-line19F-G155S (mean 3.4, SD 0.9) were greater than mock-vaccinated mice (mean 0.4, SD 0.6; $P < .005$), but less than mice vaccinated with A2-line19F-G155 (mean 6.0, SD 1.4; $P < .005$) and similar to wild-type A2-line19F (mean 4.8, SD 0.8; $P = .252$) (Supplementary Table 2).

DISCUSSION

We generated 2 RSV live-attenuated vaccine candidates with deleted G-protein mucin domains, expressing either secreted G only (A2-line19F-G155S) or both transmembrane and secreted forms of G (A2-line19F-G155). Protein expression of F and G was confirmed by western blotting and by immunofluorescence of infected HEp-2 cells using flow cytometry. Removal of the G-mucin domains significantly attenuated viral propagation in primary NHBE cells at ALI, but did not meaningfully decrease propagation in Vero cells. These results indicated that both vaccine strains, while highly attenuated in primary human airway cells, could still be propagated in Vero cells for the purpose of vaccine production.

In a mouse model, we found that A2-line19F-G155 and A2-line19F-G155S were attenuated, immunogenic, and efficacious. The vaccines were heavily attenuated by measurement of lung viral load following intranasal infection using a live-virus FFU assay. Similarly, RSV RNA in the lung, as measured

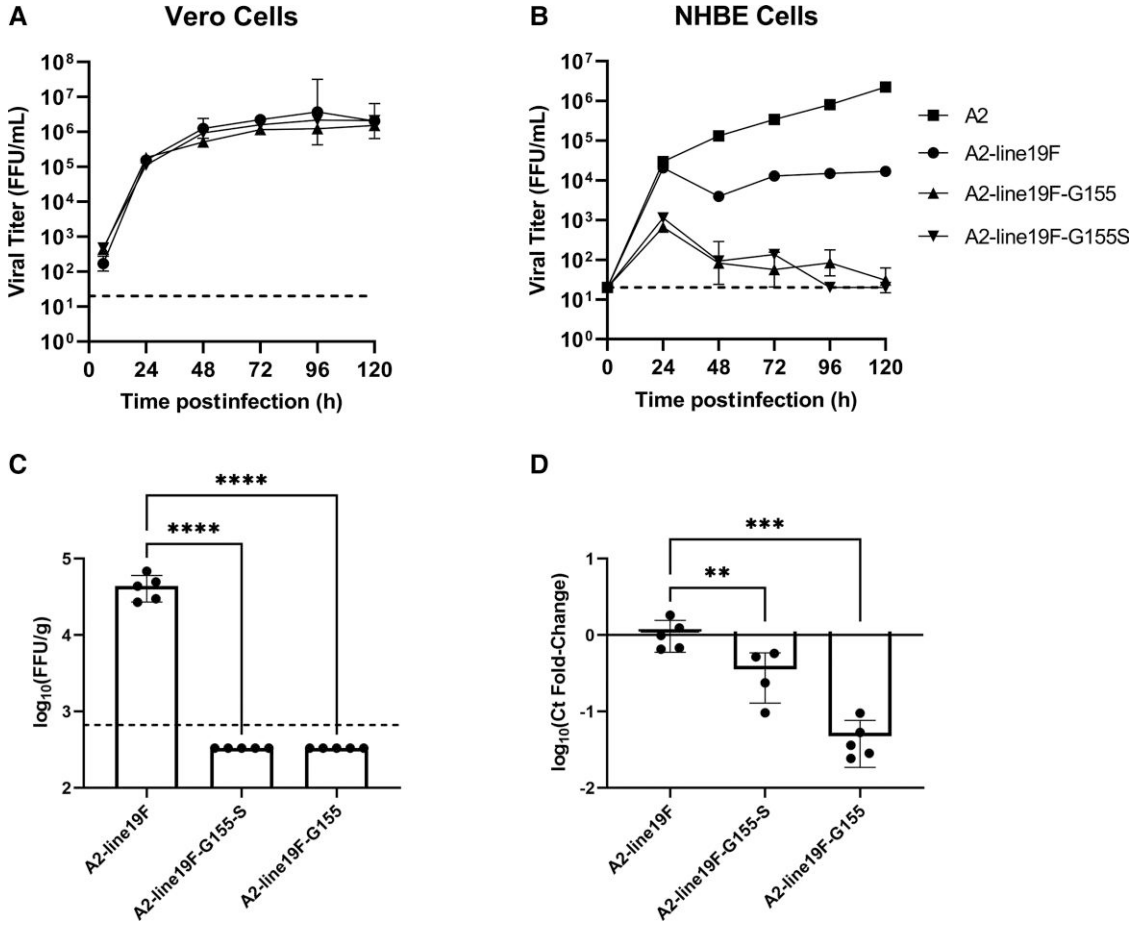

Figure 4. Viral growth kinetics of G-mutant vaccines in vitro and in BALB/c mice. *A*, Vero cells and (*B*) NHBE cells differentiated at ALI were infected with A2-line19F, A2-line19F-G155 (deleted mucin domains), A2-line19F-G155S (deleted mucin and transmembrane domains), or A2 (NHBE cells only). Data represent the geometric mean of 2 or 3 experimental replicates (± geometric SD), expressed as FFU/mL. Vaccine attenuation was measured in BALB/c mice infected intranasally on day 4 postinfection by (*C*) live-virus FFU assay or by (*D*) RT-PCR. *C*, Data represent the geometric mean titer (± geometric SD) viral lung titer in $\log_{10}$(FFU/g lung). *D*, Data represent the mean (± SD) delta-delta cycle threshold (ΔΔCt) value between *GAPDH* and RSV M gene, normalized to A2-line19F. Statistical comparisons were made using 1-way analysis of variance of log-transformed titers with Tukey post hoc comparisons test. ** $P \leq .01$, *** $P \leq .005$, and **** $P \leq .001$. Abbreviations: ALI, air-liquid interface; FFU, fluorescent focus units; *GAPDH*, glyceraldehyde-3-phosphate dehydrogenase; NHBE, normal human bronchial epithelial; RSV, respiratory syncytial virus; RT-PCR, real-time polymerase chain reaction. The dashed lines represent the lower limits of detection of the assays.

by RT-PCR was reduced by 3- and 22-fold for A2-line19F-G155S and A2-line19F-G155, respectively, compared to A2-line19F. Both vaccine candidates elicited high titers of RSV prefusion F and neutralizing antibodies, which were comparable to A2-line19F. The vaccine candidates were protective against intranasal RSV challenge in mice and did not elicit enhanced pulmonary histopathology, which is an important safety metric for RSV vaccines. In these ways, the deletion of RSV G-mucin domains conferred multiple desirable features of an RSV live-attenuated vaccine candidate, including simultaneous enhanced attenuation and retained immunogenicity in a genetically stable construct.

There is a growing body of evidence that glycosylated domains of viral glycoproteins can function as steric shields, masking surface epitopes from recognition by the host immune system and facilitating immune evasion [13, 14]. One well-characterized example of this is Ebola virus (EBOV), which expresses a large surface glycoprotein (GP) that comprises both attachment and fusion functions. EBOV GP sterically occludes epitopes within the GP itself, in addition to surface proteins of virally infected cells such as MHC1 and β1 integrin. In this way, EBOV GP impairs both antibody-mediated recognition of viral antigens and CD8 T-cell recognition of MHC1 on antigen-presenting cells. Removal of GP *N*- and *O*-linked glycans or removal of the surface subunit of GP allows for deshielding of these epitopes and immune recognition [13]. Importantly, to retain immunogenicity, the removal of surface glycans must not disrupt conformational epitopes recognized by neutralizing antibodies.

The role of glycosylation in RSV pathogenesis has been incompletely characterized. Whereas the G protein has highly variable glycosylated sites within its mucin domains, the F protein has only 5 conserved *N*-glycosylation sites [8]. Removal of

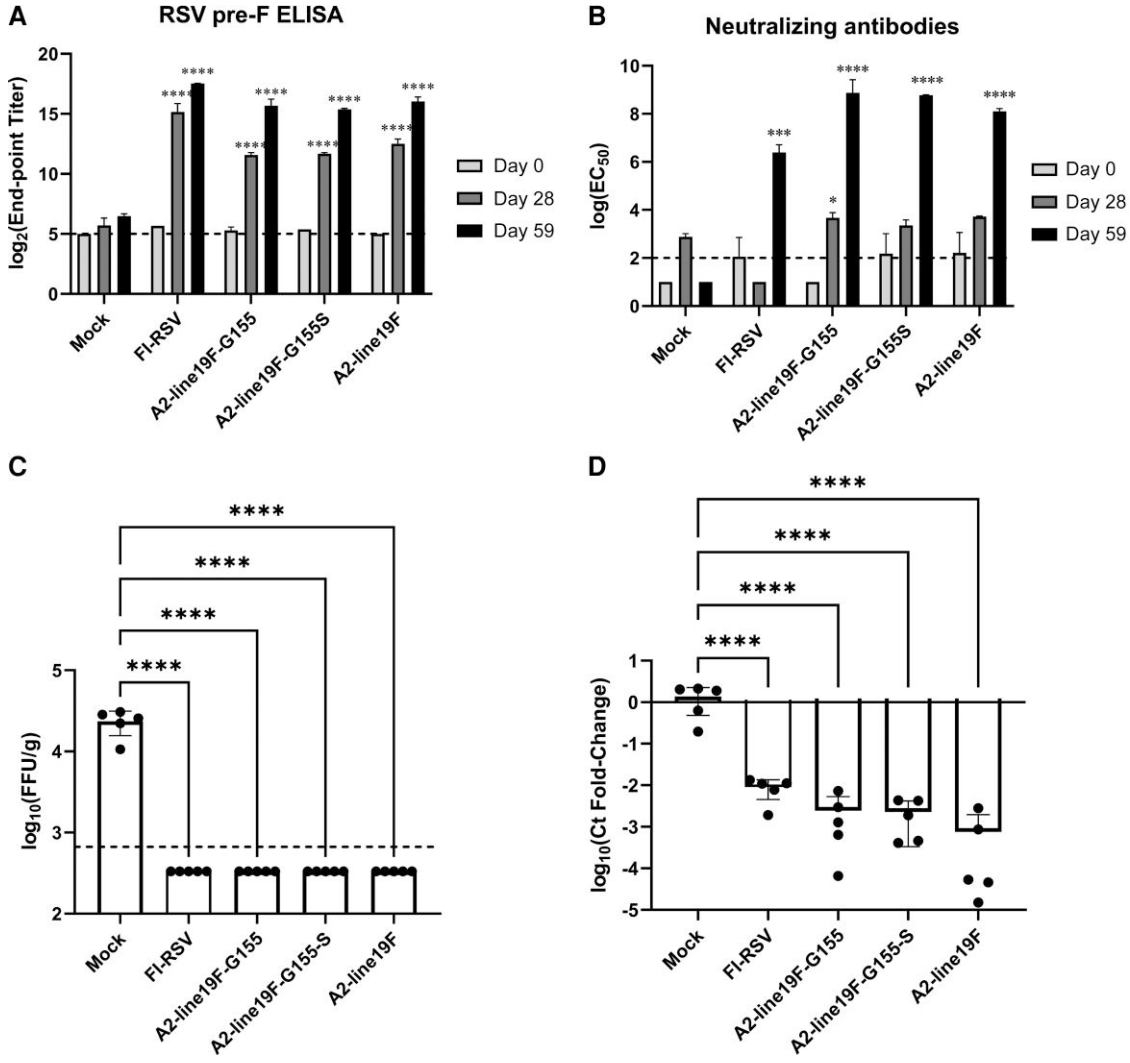

Figure 5. Immunogenicity and efficacy of G-mutant vaccines in BALB/c mice. Mice were primed and boosted on days 1 and 29, respectively. Binding and neutralizing antibody responses were measured on days 0, 28, and 59 by (*A*) RSV prefusion F ELISA, and (*B*) neutralizing antibodies to A2-line19F in HEp-2 cells. Sera from groups of mice were pooled and analyzed in 2 replicates in duplicate for ELISAs, which are expressed as $\log_2$ (end-point titers) for ELISAs and geometric means of the $\log(EC_{50})$ for neutralization assays. On day 60, mice were challenged intranasally with 10^6 FFU A2-line19F. Four days later, lungs were harvested and virus titrated by either (*C*) live-virus FFU assay or (*D*) RT-PCR. *C*, Data represent the geometric mean titer (± geometric SD) viral lung titer in $\log_{10}$(FFU/g lung). *D*, Data represent the mean (± SD) delta-delta cycle threshold (ΔΔCt) value between *GAPDH* and RSV M gene, normalized to mock. Statistical comparisons were made using 1-way analysis of variance of log-transformed titers with Tukey post hoc comparisons test. * $P \leq .05$, *** $P \leq .005$, and **** $P \leq .001$. Abbreviations: EC_{50}, 50% maximum effective concentration; ELISA, enzyme-linked immunosorbent assay; FFU, fluorescent focus unit; *GAPDH*, glyceraldehyde-3-phosphate dehydrogenase; RSV, respiratory syncytial virus; RT-PCR, real-time polymerase chain reaction. The dashed lines represent the lower limits of detection of the assays.

the F protein *N*-glycosylation sites, singly or in combination, has been shown to differentially impede fusogenicity, attenuate viral replication, and modulate immunogenicity [24]. A similar analysis has not been undertaken to date for the RSV G protein, which contains 30–40 *O*-glycosylation sites and 4–5 *N*-glycosylation sites. In this study, we found that removal of the G-mucin domains with/without the transmembrane domain did not appreciably affect viral expression of F protein by western blotting, but did reduce monoclonal antibody binding to F by whole-virus ELISA, suggestive of F deshielding. Nevertheless, the differences between monoclonal antibody binding to the surface of infected HEp-2 cells as measured by flow cytometry were modest, and future studies are needed to confirm the mechanism of retained immunogenicity in these highly attenuated constructs. As recent studies have demonstrated that G produced in primary human bronchial epithelial cells is much more heavily glycosylated (170 kDa) than G produced in immortalized cell lines (95 kDa) [25], it is likely that the effects of mucin domain deletion on epitope deshielding is more pronounced in human airway cells than in HEp-2 cells.

Limitations of this study include the utilization of a single animal model, BALB/c mice, which is insufficient to fully

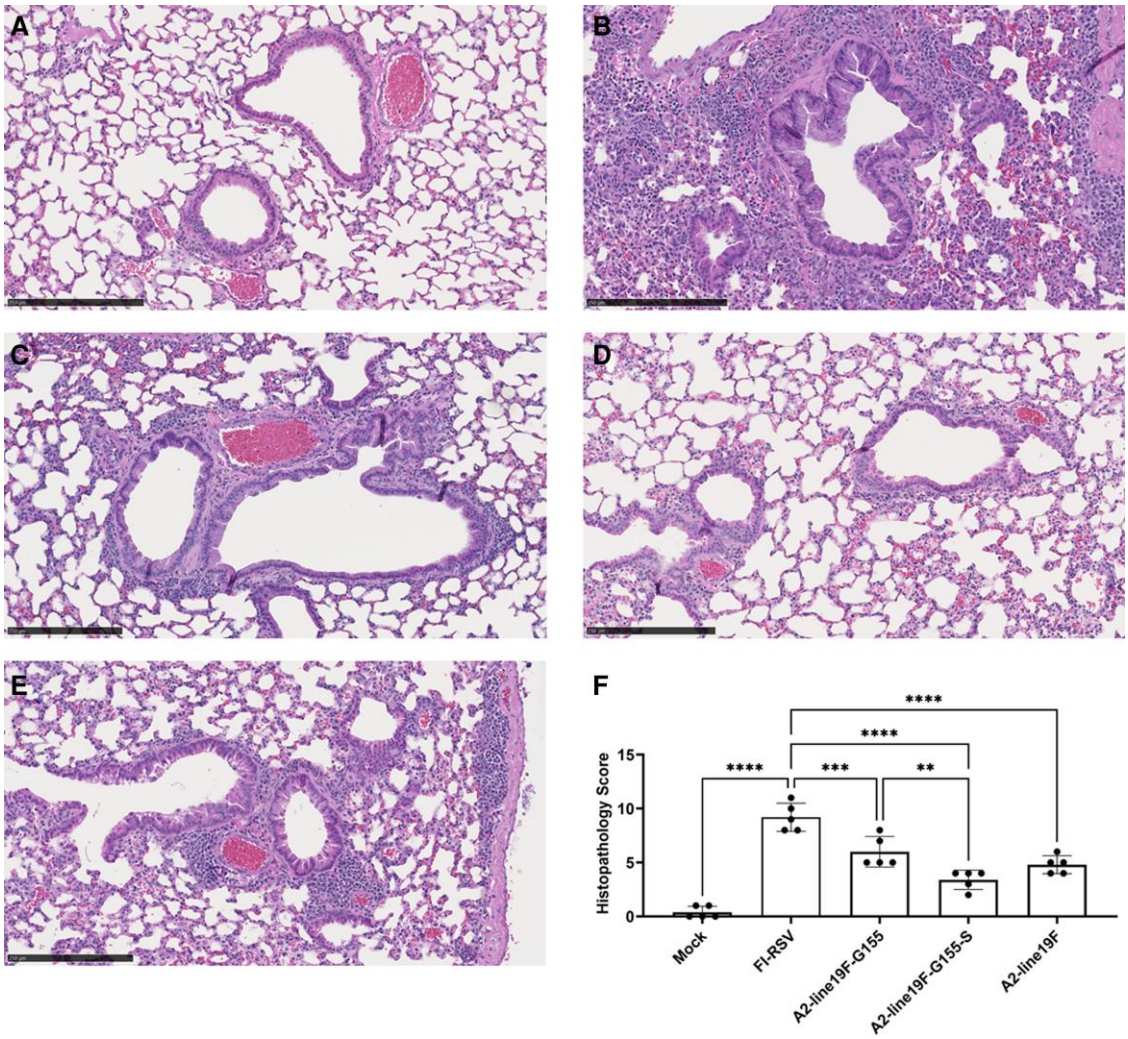

Figure 6. Lung histopathology in immunized mice after A2-line19F challenge. Groups of 5 BALB/c mice were vaccinated with (*A*) mock (plain minimum essential medium [MEM]), (*B*) formalin-inactivated RSV (FI-RSV) intramuscular, or 10^6 fluorescent focus unit (FFU) intranasally of (*C*) A2-line19F-G155, (*D*) A2-line19F-G155S, or (*E*) A2-line19F. On day 60 postvaccination, mice were challenged intranasally with 10^6 FFU A2-line19F. Four days later, the lungs were harvested for hematoxylin-eosin staining and (*F*) histopathological scoring. Representative images are shown. Scale bar = 250 µm. Data represent mean histopathological scores ± SD. Statistical comparisons were made using 1-way analysis of variance with Tukey post hoc comparisons test. ** $P \leq .01$, *** $P \leq .005$, and **** $P \leq .001$.

recapitulate human pathogenesis and immune responses. The cellular immune responses and the breadth and durability of protective immunity also were not assessed. We also only analyzed the effects of deleting the G-mucin domains in 1 strain of RSV (A2-line19F). Whether removal of these highly variable domains might improve the breadth of immune responses by unmasking conserved epitopes is an area of future study. Although the A2-line19F-G155 vaccine candidate had complete sequence identity to the generated strain, the A2-line19F-G155S acquired a single point mutation in the L protein, underscoring one inherent challenge of developing live-attenuated vaccines for RNA viruses. Histopathological analyses were performed on day 4 postchallenge in this study to optimize viral detection by FFU assay and RT-PCR, preceding the usual timing of peak histopathological changes observed in mice after RSV infection (day 6). This may explain the low histopathology scores observed in mock-vaccinated mice after initial RSV exposure and challenge. Future analyses should address these considerations in more permissive animal models, such as cotton rats or nonhuman primates.

In conclusion, we generated RSV LAV candidates lacking G-protein mucin domains, which were highly attenuated with retained immunogenicity in BALB/c mice. Deglycosylation of viral glycoproteins may represent a novel strategy to balance LAV attenuation and immunogenicity through deshielding of surface epitopes.

Supplementary Data

Supplementary materials are available at *The Journal of Infectious Diseases* online. Consisting of data provided by the

authors to benefit the reader, the posted materials are not copy-edited and are the sole responsibility of the authors, so questions or comments should be addressed to the corresponding author.

Notes

Acknowledgments. Purified prefusion F protein for ELISAs was kindly provided by Meissa Vaccines, Inc. 3D3 was kindly provided by Lawrence Kauvar, Tellis Bioscience, LLC. Motavizumab was kindly provided by MedImmune, Inc. We thank Vaunita Parihar and the Emory Cancer Tissue and Pathology Core Facility for preparing the histopathological specimens.

Financial support. This work was supported by the Center for Childhood Infections and Vaccines at Emory University and Children's Healthcare of Atlanta; and by the Pediatric Infectious Diseases Society Pichichero Family Foundation for Vaccine Development Research Award.

Potential conflicts of interest. M. L. M. is an employee and shareholder of Meissa Vaccines. E. J. A. has consulted for Pfizer, Sanofi Pasteur, Janssen, GSK, and Medscape; and serves on data and safety monitoring boards for Kentucky BioProcessing, Inc, and Sanofi-Pasteur. His institution receives funds to conduct clinical research unrelated to this work from MedImmune, Regeneron, PaxVax, Pfizer, GSK, Merck, Sanonfi-Pasteur, Janssen, and Micron; and has received funding from National Institutes of Health (NIH) to conduct clinical trials of Moderna and Janssen COVID-19 vaccines. C. A. R.'s institution has received funding to conduct clinical research unrelated to this work from BioFire Inc, GSK, MedImmune, Micron, Merck, Novavax, PaxVax, Regeneron, Pfizer, and Sanofi-Pasteur; and funding from NIH to conduct clinical trials of Moderna and Janssen COVID-19 vaccines. C. A. R. and C. S. S. are coinventors of patented RSV vaccine technology, which has been licensed to Meissa Vaccines, Inc. L. J. A. has done paid consultancies on RSV vaccines for Bavarian Nordic, ClearPath Vaccines Company, Janssen, Pfizer, and ADVI; is a coinventor on several Centers for Disease Control and Prevention patents on the RSV G protein and its CX3C chemokine motif relative to immune therapy and vaccine development; is coinventor on a patent filing for use of RSV platform VLPs with the F and G proteins for vaccines; and his laboratory is currently receiving funding through Emory University from Pfizer for laboratory studies for RSV surveillance studies in adults, Sciogen for animal studies of RSV vaccines, and Advaccine Pharmaceuticals, Ltd for RSV neutralizing antibody studies. All other authors report no potential conflicts. M. K. R., S. A. L., E. J. A., L. J. A., C. S. S., and C. A. R. are co-inventors of the vaccine technology described herein, which has been submitted for a provisional patent by Emory University.

All authors have submitted the ICMJE Form for Disclosure of Potential Conflicts of Interest. Conflicts that the editors consider relevant to the content of the manuscript have been disclosed.

References

1. Andeweg SP, Schepp RM, van de Kassteele J, Mollema L, Berbers GAM, van Boven M. Population-based serology reveals risk factors for RSV infection in children younger than 5 years. Sci Rep **2021**; 11:8953.
2. Li Y, Wang X, Blau DM, et al. Global, regional, and national disease burden estimates of acute lower respiratory infections due to respiratory syncytial virus in children younger than 5 years in 2019: a systematic analysis. Lancet **2022**; 399:2047–64.
3. Agha R, Avner JR. Delayed seasonal RSV surge observed during the COVID-19 pandemic. Pediatrics **2021**; 148: e2021052089.
4. Kim HW, Canchola JG, Brandt CD, et al. Respiratory syncytial virus disease in infants despite prior administration of antigenic inactivated vaccine. Am J Epidemiol **1969**; 89:422–34.
5. Wright PF, Karron RA, Belshe RB, et al. The absence of enhanced disease with wild type respiratory syncytial virus infection occurring after receipt of live, attenuated, respiratory syncytial virus vaccines. Vaccine **2007**; 25:7372–8.
6. Stobart CC, Rostad CA, Ke Z, et al. A live RSV vaccine with engineered thermostability is immunogenic in cotton rats despite high attenuation. Nat Commun **2016**; 7:13916.
7. Rostad CA, Stobart CC, Gilbert BE, et al. A recombinant respiratory syncytial virus vaccine candidate attenuated by a low-fusion F protein is immunogenic and protective against challenge in cotton rats. J Virol **2016**; 90:7508–18.
8. McLellan JS, Ray WC, Peeples ME. Structure and function of respiratory syncytial virus surface glycoproteins. Curr Top Microbiol Immunol **2013**; 372:83–104.
9. Pandya MC, Callahan SM, Savchenko KG, Stobart CC. A contemporary view of respiratory syncytial virus (RSV) biology and strain-specific differences. Pathogens **2019**; 8:67.
10. Kishko M, Catalan J, Swanson K, et al. Evaluation of the respiratory syncytial virus G-directed neutralizing antibody response in the human airway epithelial cell model. Virology **2020**; 550:21–6.
11. Bukreyev A, Yang L, Fricke J, et al. The secreted form of respiratory syncytial virus G glycoprotein helps the virus evade antibody-mediated restriction of replication by acting as an antigen decoy and through effects on Fc receptor-bearing leukocytes. J Virol **2008**; 82:12191–204.
12. Tripp RA, Power UF, Openshaw PJM, Kauvar LM. Respiratory syncytial virus: targeting the G protein provides a new approach for an old problem. J Virol **2018**; 92:e01302.
13. Francica JR, Varela-Rohena A, Medvec A, Plesa G, Riley JL, Bates P. Steric shielding of surface epitopes and impaired immune recognition induced by the Ebola virus glycoprotein. PLoS Pathog **2010**; 6:e1001098.

14. Lennemann NJ, Rhein BA, Ndungo E, Chandran K, Qiu X, Maury W. Comprehensive functional analysis of N-linked glycans on Ebola virus GP1. MBio **2014**; 5:e00862-13.
15. Rostad CA, Stobart CC, Todd SO, et al. Enhancing the thermostability and immunogenicity of a respiratory syncytial virus (RSV) live-attenuated vaccine by incorporating unique RSV Line19F protein residues. J Virol **2018**; 92: e01568.
16. Hotard AL, Shaikh FY, Lee S, et al. A stabilized respiratory syncytial virus reverse genetics system amenable to recombination-mediated mutagenesis. Virology **2012**; 434:129–36.
17. Morgan R, Manfredi C, Easley KF, et al. A medium composition containing normal resting glucose that supports differentiation of primary human airway cells. Sci Rep **2022**; 12:1540.
18. Stobart CC, Hotard AL, Meng J, Moore ML. Reverse genetics of respiratory syncytial virus. Methods Mol Biol **2016**; 1442:141–53.
19. Cao D, Gao Y, Roesler C, et al. Cryo-EM structure of the respiratory syncytial virus RNA polymerase. Nat Commun **2020**; 11:368.
20. Jumper J, Evans R, Pritzel A, et al. Highly accurate protein structure prediction with AlphaFold. Nature **2021**; 596:583–9.
21. Kelley LA, Mezulis S, Yates CM, Wass MN, Sternberg MJ. The Phyre2 web portal for protein modeling, prediction and analysis. Nat Protoc **2015**; 10:845–58.
22. Hotard AL, Lee S, Currier MG, et al. Identification of residues in the human respiratory syncytial virus fusion protein that modulate fusion activity and pathogenesis. J Virol **2015**; 89:512–22.
23. Wright PF, Ikizler MR, Gonzales RA, Carroll KN, Johnson JE, Werkhaven JA. Growth of respiratory syncytial virus in primary epithelial cells from the human respiratory tract. J Virol **2005**; 79:8651–4.
24. Leemans A, Boeren M, Van der Gucht W, et al. Characterization of the role of N-glycosylation sites in the respiratory syncytial virus fusion protein in virus replication, syncytium formation and antigenicity. Virus Res **2019**; 266:58–68.
25. King T, Mejias A, Ramilo O, Peeples ME. The larger attachment glycoprotein of respiratory syncytial virus produced in primary human bronchial epithelial cultures reduces infectivity for cell lines. PLoS Pathog **2021**; 17:e1009469.